Geoderma 272 (2016) 32–38

Contents lists available at ScienceDirect

Geoderma

journal homepage: www.elsevier.com/locate/geoderma

Distribution and geochemical speciation of soil mercury in Wanshan Hg mine: Effects of cultivation

Runsheng Yin [a,b,c], Chunhao Gu [a], Xinbin Feng [a,*], James P. Hurley [c,d], David P. Krabbenhoft [e], Ryan F. Lepak [c], Wei Zhu [a], Lirong Zheng [f], Tiandou Hu [f]

[a] State Key Laboratory of Environmental Geochemistry, Institute of Geochemistry, Chinese Academy of Sciences, Guiyang 550002, China
[b] State Key Laboratory of Ore Deposit Geochemistry, Institute of Geochemistry, Chinese Academy of Sciences, Guiyang 550002, China
[c] Environmental Chemistry and Technology Program, University of Wisconsin–Madison, Madison, WI 53706, USA
[d] Department of Civil and Environmental Engineering, University of Wisconsin–Madison, Madison, WI 53706, USA
[e] U.S. Geological Survey, 8505 Research Way, Middleton, WI 53562, USA
[f] Beijing Synchrotron Radiation Facility, Institute of High Energy Physics, Chinese Academy of Sciences, Beijing 100049, China

ARTICLE INFO

Article history:
Received 20 April 2015
Received in revised form 20 January 2016
Accepted 3 March 2016
Available online 12 March 2016

Keywords:
Mercury
Soil
Distribution
Speciation
XANES
Cultivation

ABSTRACT

The distribution and speciation of mercury (Hg) were investigated in contaminated soils collected from two adjacent land use systems (arid land and rice paddy) near the Wanshan Mercury mine, SW China. In both sites, fine soil aggregate size fractions (<231 μm) showed higher total Hg concentrations and higher soil organic matter contents than in larger aggregate size fractions (231 to 2000 μm). Compared to arid land, paddy soils are characterized by higher proportions of fine soil aggregates, higher soil organic matter and higher total Hg content. Soil Hg speciation, based on X-ray absorption spectroscopy (XANES) analysis, indicated that the majority (64–81%) of Hg in soils under both land use systems was associated with metacinnabar (β-HgS), indicating the precipitation of β-HgS in soils. We also observed the presence of bioavailable $HgCl_2$ and Hg(0) in soils at both sites, which may represent a considerable environmental concern. Our study clearly showed that different cultivation practices can largely change the distribution and speciation of Hg in agriculture soils.

1. Introduction

Mercury (Hg) is an important pollutant due to its global distribution, bioaccumulation and toxicity (Yin et al., 2014). Mercury contamination is a widespread problem due to the increasing anthropogenic emissions and deposition of Hg to soils (Li et al., 2009; Yin et al., 2012). The mobility, bioavailability and toxicity of Hg in soils are strongly dependent on chemical speciation (Stein et al., 1996). Mining sites are "hotpots" of soil Hg contamination. The roasting process (500–800 °C) during Hg refining liberates elemental Hg(0) from Hg ores (Yin et al., 2013a) and produces gangue materials and waste calcines. Like Hg ores, gangue materials mainly contain cinnabar (α-HgS) and waste calcines contain secondary Hg phases such as metacinnabar (β-HgS), mercuric chloride ($HgCl_2$), Hg sulfates, and Hg oxides (Kim et al., 2000). In Hg mining areas, soil contamination is mainly derived by leaching Hg from tailings and deposition of Hg(0) emitted from the roasting facilities and tailings. Studies of speciation of Hg in soils from mining-impacted areas have identified mainly mercuric sulfides with minor Hg salts (e.g., $HgCl_2$) and Hg(0) present (Schuster, 1991; Fernández-Martínez et al., 2006; Rimondi et al., 2014). Soluble Hg salts are more easily transported and typically serve as the substrate for Hg(II) reduction and methylation during various biological and abiotic processes. Methylmercury (MeHg) only represent a small fraction of the total Hg in soils, whereas it is a more toxic species and can be bioaccumulated in the food chains (Akagi and Nishimura, 1991).

The Wanshan Mercury Mine District (WMMD) is the largest historic Hg-producing district in China (Fig. 1). Long-term mining activities in WMMD have produced roughly 125.8 million tons of mine wastes, which are mainly consisted of the roasted calcines and gangue materials (Jiang et al., 2006). Mercury in mine waste has been eroded and transported to local soils (Zhang et al., 2004; Qiu et al., 2005). Contaminated soils in WMMD in turn are currently being utilized in paddy rice and arid land cropping practices (e.g. corn) (Qiu et al., 2008). This integrated cropping system has the potential to create changes in the physical, chemical and bacterial properties of the soil, which may affect the distribution and speciation of Hg, and potentially cause differences in MeHg production in the soils (Roulet et al., 1998, 1999; Farella et al., 2007). Relatively high levels of MeHg have been reported in rice paddies compared to arid land cropping soils (Kelly et al., 1997; Rothenberg et al., 2011). A recent study in WMMD demonstrated much higher MeHg concentrations in rice (up to 100 μg kg^{-1}), 10–100 fold higher than that of other arid land plants (e.g. corn, conola, tobacco and cabbage) (Qiu et al., 2008). Understanding the effect of contrasting

* Corresponding author.
E-mail address: fengxinbin@vip.skleg.cn (X. Feng).

http://dx.doi.org/10.1016/j.geoderma.2016.03.003
0016-7061/

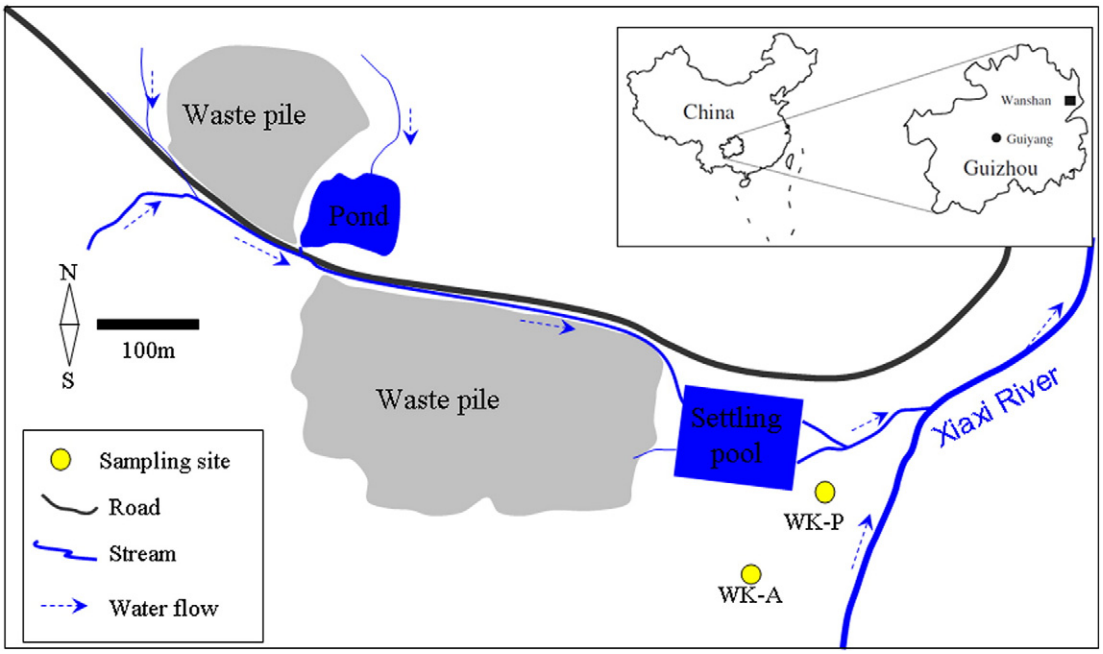

Fig. 1. Sampling locations of sites in the Wanshan Mercury Mining District.

cultivation practices on soil Hg distribution and speciation is important in evaluating food Hg safety.

Chemical speciation of Hg in solids has been investigated using sequential extraction (Chadwick et al., 2013), solid-phase-Hg-thermo-desorption (Biester et al., 1999) and X-ray absorption spectroscopy (XANES) (Kim et al., 2000; Gray et al., 2004, 2006; Jew et al., 2010). Among those methods, XANES is well known by its direct and non-destructive advantages (Kim et al., 2000; Gray et al., 2004, 2006; Jew et al., 2010). Utilizing XANES, our previous study reported large differences in Hg speciation in two of the most important Hg contamination sources, roasted calcines and unroasted Hg ore, in WMMD (Yin et al., 2013a, 2013b, 2013c). However, contaminated soils in WMMD with different agricultural cultivation practices have not been investigated by XANES. This study then investigated the hypothesis that an alternating sequence of paddy rice and dry land cropping will affect changes in the distribution and speciation of Hg in soil. Soil samples collected from both rice and arid land cropping farmlands in WMMD were analyzed for total Hg (THg) and utilized EXAFS analysis to understand speciation and the relationship to cultivation practices in this historically-contaminated Hg mining region.

2. Materials and methods

2.1. Study sites and sampling

The WMMD is located in Guizhou Province, SW China (Fig. 1). Large-scale mining activities ceased at WMMD in 2001. Due to long-term Hg mining activities during the past hundreds of years, Hg waste tailings are widespread (Jiang et al., 2006), and leading to serious Hg contamination of the surrounding environment (Zhang et al., 2004; Qiu et al., 2005, 2008; Zhang et al., 2010; Yin et al., 2013a, 2013b, 2013c). This study chose sites near the Wukeng (WK) pile, which is seated at the head of the Xiaxi Stream, due to its proximity to two adjacent farmlands (sites WK-P and WK-A). The WK-P is a paddy field which is used for rice planting using water from upstream on the Xiaxi stream. The WK-A site, with a relative higher elevation (~4 m higher) than the WK-P, is a dry cropping farmland used mainly for corn.

At each site, approximately 2 kg of composite soil was collected into plastic bags prior to the laboratory processing. In the laboratory, soil samples were air dried, gently crushed to disaggregate larger clumps (which did not significantly alter the aggregate size distribution), and sieved through a 2 mm nylon sieve to remove stones, coarse materials, and other debris. Samples were then stored in polyethylene bags. A portion of the sieved soils were ground to <150 μm by an agate grinder for THg analysis of the bulk soils.

2.2. Sieve analysis for soil aggregate size distribution

Approximately 500 g of the remaining air-dried 2-mm sieved soils was weighed and progressively passed through nine sieves (with 10, 20, 40, 60, 80, 120, 140, 180 and 200 mesh) (Gee and Bauder, 1986). The bulk soil samples were then separated into nine aggregate size fractions: 2000–850 μm (midpoint: 1425.0 μm), 850–389 μm (midpoint: 619.5 μm), 389–231 μm (midpoint: 310.0 μm), 231–180 μm (midpoint: 205.5 μm), 180–125 μm (midpoint: 152.5 μm), 125–105 μm (midpoint: 115.0 μm), 105–90 μm (97.5), 90–75 μm (midpoint: 82.5 μm) and <74 μm (midpoint: 37.5 μm). The weight of each aggregate size fraction was recorded and the loss of sample mass during the separation processes was no more than 2% of the total mass. The mass percentage of each aggregate size fraction within the bulk soil was calculated. Sieved soil fractions were then homogenized using a ZrO_2 homogenizer (01467-AB, SPI Supplies®), and stored in plastic bags for soil organic matter (SOM) content, THg concentration and Hg speciation analysis.

2.3. Soil organic matter content and total mercury concentration analysis

SOM contents in all sieved soil fractions were determined by reduction of Cr_2O_7(-II) by organic C and subsequent determination of unreduced Cr_2O_7(-II) by oxido-reduction titration with Fe(II) (Nelson and Sommers, 1982). THg in bulk soil and soil size fractions were analyzed by a Lumex RA 915$^+$ Hg analyzer (Lumex Ltd., Russia). The detection limit for THg was 0.5 ng g^{-1}. Quality control for THg analysis was addressed using certified reference material (NIST SRM 2710, Montana Soil I), with an average recovery of 98.0 ± 1.4% (2σ, n = 5). The enrichment factors (EFs) of Hg in each aggregate size fraction with respect to bulk soil was calculated as $EF = THg_{fraction}/THg_{bulk}$, where $THg_{fraction}$ and THg_{bulk} were the concentrations of THg in a given aggregate size fraction and the bulk soil sample, respectively.

2.4. Mercury speciation analysis using XANES

Speciation of Hg in different soil aggregate size fractions was determined by mercury L_{III}-edge (12.284 keV) X-ray absorption spectra at the 1W1B beamline of the Beijing Synchrotron Radiation Facility (BSRF, Beijing, China). Mercury L_{III}-edge X-ray absorption spectra were collected using a Si (111) double crystal monochromator (detuned approximately 30% to eliminate higher order harmonics). The storage ring operated at 2.2 GeV with a beam current of approximately 80 mA. An energy range of 200 to 1000 eV was used to acquire spectra. Data of all samples were collected in fluorescence mode under ambient conditions and data for reference compounds were collected in transmission mode. An average of three scans was performed to achieve an adequate signal/noise ratio (Lv et al., 2012). Although Hg has a strong affinity to organic matters, previous studies have shown that Hg in soils mainly exists as inorganic forms (Schuster, 1991). Studies indicate that organic material can inhibit crystallization and growth of HgS aggregates and stabilize colloidal HgS phases (Ravichandran et al., 1999; Deonarine and Hsu-Kim, 2009). Evidences have shown that Hg is likely to react with thiol sulfur ligands of macromolecular SOM to form Hg–SOM complexes, which is readily to convert to Hg sulfides (Manceau et al., 2015). A study on the speciation of Hg using Tessier sequential extraction procedure reported that organic bound Hg only constitute <20% of the THg in WMMD soils (Bao et al., 2011). Skyllberg (2008) showed that inorganic sulfide–Hg(II)-complexes can predominate over Hg(II)-thiols even in a peat soil with 50% organic content. In this study, investigation of the potential components and chemical structures of the samples are mainly inorganic compounds including elemental Hg(0), cinnabar (α-HgS), meta-cinnabar (β-HgS), mercuric chloride ($HgCl_2$), mercuric sulfate ($HgSO_4$), yellow mercuric oxide (yellow HgO), red mercuric oxide (red HgO), mercuric acetate ($Hg(Ac)_2$) and mercuric selenide (HgSe). Elemental Hg(0) is a liquid and thus disordered at ambient-temperature and pressure (Jew et al., 2010). Crystalline Hg(0) at (77 K) temperatures were used to quantify the Hg(0) fraction during the XANES analysis (Jew et al., 2010). Instead of using a low temperature technique, we show that it is possible to quantify Hg(0) by regulating the liquid Hg(0) into Hg-purged solid phase using the following procedure: 1) purging Hg from a ground mine calcine sample (<150 μm) from WMMD using a muffle furnace (550 °C, 12 h); 2) mixing liquid Hg(0) from a broken thermometer (containing approximately 0.7 g Hg) with 100 g Hg-free calcine powder in a sealed glass bottle for 24 h. THg concentrations in the unpurged and Hg-free calcine sample were 52 μg g^{-1} and 29 ng g^{-1}, respectively. The XANES spectra of both samples and standards are shown in Fig. 2. Linear combination fits (LCF) to all the Hg spectra were performed by the whole reference components through Athena program in the IFEFFIT package (Newville, 2001). The XANES spectrum collected from a natural sample containing multiple Hg phases can be decomposed using a linear least-squares fitting method into the sum of its individual standard compound, through direct comparison with the model compound spectra. Fitting results of the composition of each sample are constrained by the definition to only those library reference compounds.

3. Results

3.1. Soil aggregate size distribution and soil organic matter content

The average mass distribution of different soil aggregate size fractions in both WK-A and WK-P is given in Table 1. The fractioned bulk masses in both WK-A and WK-P gradually decreases with decreasing aggregate sizes (Fig. 3A). Similar patterns of soil aggregate size distribution have been reported by many studies (Gee and Bauder, 1986; Hardy and Cornu, 2006). In WK-A, the largest soil aggregate size fraction is 2000–850 μm (37.15%), followed by 850–389 μm (24.45%), 389–231 μm(11.99%), 231–180 μm (8.02%), 180–125 μm (6.11%), 125–105 μm (4.79%), 105–90 μm (3.69%), 90–74 μm (2.64%) and <74 μm (1.17%). In WK-P, the largest soil aggregate size fraction is 2000–850 μm (24.68%), followed by 850–389 μm (20.10%), 389–231 μm (14.58%), 231–180 μm (12.18%), 180–125 μm (9.80%), 125–105 μm (7.45%), 105–90 μm (4.96%), 90–74 μm (3.40%) and <74 μm (2.84%). The SOM contents in WK-A and WK-P in different aggregate size fractions range from 4 to 22 mg g^{-1} and 8 to 33 mg g^{-1}, respectively (Table 1 and Fig. 3B). In general, the SOM contents in both WK-A and WK-P soils increase with the increase of soil aggregate sizes (Fig. 3B), consistent with other observations of Hg in fine-grained agricultural soils (Schmidt and Kögel-Knabner, 2002).

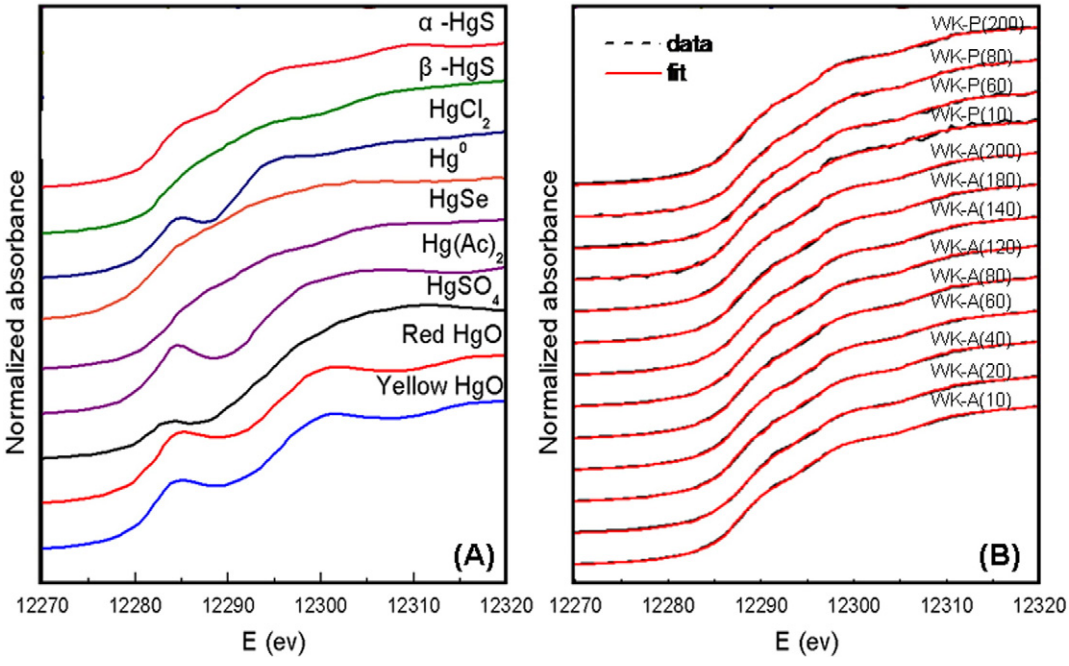

Fig. 2. XANES spectra of the reference materials (A) and samples (B).

Table 1
Aggregate size distribution, soil organic matter content, total mercury and mercury speciation in soils from selected sites in the Wanshan Mercury Mining District.

Sampling site	Aggregate size range (μm)	Midpoint (μm)	Mass (%)	SOM (mg g^{-1})	Fractional SOM (%)	THg (μg g^{-1})	Fractional Hg (%)	EF	β-HgS (%)	α-HgS (%)	$HgCl_2$ (%)	Hg(0) (%)
WK-A	2000–850	1425.0	37.2	4	20.0	125.3	33.1	0.89	76.6	2.4	9.3	12.9
	850–389	619.5	24.5	5	16.5	133.6	23.2	0.95	75.7	3.6	5.4	15.6
	389–231	310.0	12.0	8	12.9	150.5	12.8	1.07	76.0	2.0	7.4	16.5
	231–180	205.5	8.0	10	10.8	150.3	8.6	1.07	73.6	1.6	12.5	13.7
	180–125	152.5	6.1	13	10.7	151.8	6.6	1.08	79.1	2.0	9.0	12.6
	125–105	115.0	4.8	18	11.6	164.3	5.6	1.17	74.8	2.0	10.3	15.5
	105–90	97.5	3.7	13	6.5	171.5	4.5	1.22	76.5	2.4	12.7	9.5
	90–75	82.5	2.6	22	7.8	196.3	3.7	1.40	73.1	3.9	10.7	14.1
	<75	37.5	1.2	21	3.3	221.3	1.8	1.57	70.3	6.7	10.4	14.3
WK-P	2000–850	1425.0	24.7	8	11.6	200.5	21.4	0.87	68.4	7.0	1.4	23.2
	850–389[a]	619.5	20.1	13	15.4	198.0	17.2	0.86	–	–	–	–
	389–231[a]	310.0	14.6	17	14.6	225.0	14.2	0.97	–	–	–	–
	231–180	205.5	12.2	23	16.5	209.5	11.0	0.90	70.2	16.4	9.0	4.4
	180–125[a]	152.5	9.8	20	11.6	246.5	10.4	1.06	–	–	–	–
	125–105[a]	115.0	7.5	26	11.4	221.0	7.1	0.95	–	–	–	–
	105–90[a]	97.5	5.0	23	6.7	295.7	6.3	1.28	–	–	–	–
	90–75	82.5	3.4	33	6.6	466.8	6.9	2.02	72.0	9.2	7.1	12.3
	<75	37.5	2.8	33	5.5	447.3	5.5	1.93	67.4	11.6	5.9	16.7

[a] Sample not analyzed by XANES.

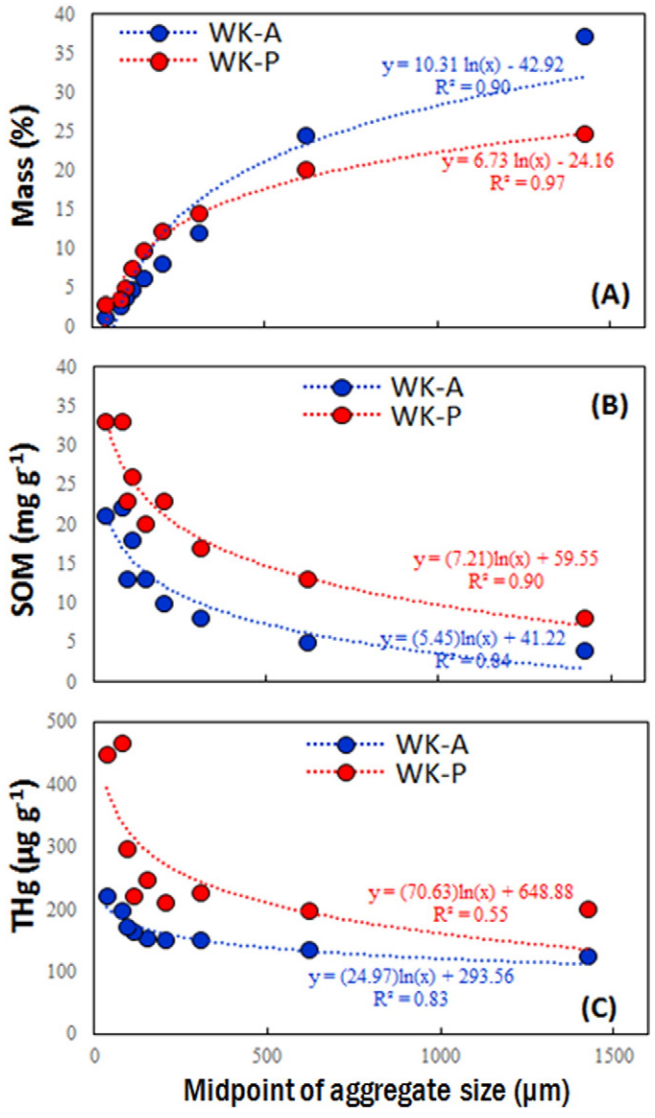

Fig. 3. Mass fractions (A), SOM (B), and THg (C) concentrations of the sieved soil fractions from sites in the Wanshan Mercury Mining District.

3.2. Total mercury concentration

The THg_{bulk} concentrations in WK-A and WK-P are 141 μg g^{-1} and 232 μg g^{-1}, respectively. The Hg concentration in the sieved soil fractions in WK-A (125.3–221.3 μg g^{-1}) and WK-P (198.0–466.8 μg g^{-1}) are given in Table 1. All samples exceed the limit value (23 μg g^{-1}) of inorganic Hg for residential soil set by USEPA (2011), indicating a high environmental risk related to crop safety. As shown in Fig. 3C, both sites show increasing patterns of THg along with the decrease of aggregate size. Mercury tended to accumulate in the fine fractions, which can be indicated more clearly by the EFs. The EFs of THg in different size classes demonstrated higher accumulation in finer fractions (Table 1), which is in line with previous reports on the preferential partitioning of Hg to fine soil fractions (Fernández-Martínez et al., 2006).

3.3. Mercury speciation

Most XANES fitting studies allow errors of 10% of their stated value (Kim et al., 2004). In this study, single-component fits were first attempted in order to identify significant contributors (i.e., ≥10% of the overall spectrum) to the final fit. This subset of significant components was then used to generate two-component fits, repeating the process until no more significant contributors could be identified. Principal component analysis/target transform helps validate the identification of four components in fitting the results (Table 1). Some spectra contribute in <10% amounts that they may be statistically insignificant, however.

As shown in Table 1, four Hg phases can be identified in the investigated samples: α-HgS, β-HgS, $HgCl_2$ and Hg(0). These phases are classified as contributing to the overall fit and the relative proportions in which they contribute, scaled to 100%, represent the final speciation of Hg in the sample. The majority of Hg in soils of WK-A (range: 69–81%) and WK-P (64–73%) is associated with β-HgS (Table 1). With the exception of two samples in WK-P (231–180 μm: 16.4%; <75 μm: 11.6%), the fractions of α-HgS in soils of WK-A and WK-P are in general lower than the analytical error (10%), and are therefore considered to be statistically insignificant. In WK-A, fine aggregate size soils (231–180 μm: 12.5%; 125–105 μm: 10.3%; 105–90 μm: 12.7%; 90–75 μm: 10.7%; <75 μm: 10.4%) contain detectable $HgCl_2$ fractions, whereas soil aggregates in WK-P have fractions of $HgCl_2$ less than 10%. In most of the samples in WK-A (except 105–90 μm: 9.5%) and WK-P (except 389–231 μm: 4.4%), detectable Hg(0) of >10% were observed. Our results are generally agreed with the XANES data reported by Rimondi et al. (2014), which

observed detectable $HgCl_2$ and Hg(0) in sediments from the Mt. Amiata Hg mine (Italy).

4. Discussion

4.1. Effects of cultivation on soil aggregate size distribution and SOM contents

Considerable differences in aggregate size distribution were observed between WK-A and WK-P soils (Fig. 3A). Soil aggregates with aggregate size ranges from 2000 to 231 μm constitute 74% and 59% of the total soil mass in WK-A and WK-P, respectively. Compared to the WK-A, the WK-P is relatively depleted in large soil aggregates (size: 2000–389 μm), whereas relatively enriched in fine soil aggregates with aggregate size <389 μm (Table 1 and Fig. 3A). Soil aggregate size distribution is reflective of the impact of soil and crop management practices (Hussain et al., 1999). Evidence that soil aggregate size distribution can be influenced by crop types, as well as soil management practices, has been reported (Arshad and Coen, 1992). Rice is often grown on soils which have a medium to fine aggregate size distribution in their surface horizon (Moormann and Breemen, 1978). This could be caused by flooding, which tends to break down larger aggregates or that larger aggregates are preferentially eroded from paddies. Rapid wetting of a dry soil have shown to cause slaking of the soil into microaggregates (Dexter, 1988). Slower rates of wetting can produce partial slaking or mellowing, which can result in considerable strength reductions and can increase the soil friability (Utomo and Dexter, 1981).

In this study, we showed that SOM is not homogeneously distributed among different aggregate size fractions (Table 1), suggesting the influence of soil texture on the partitioning of SOM in WMMD soils. Most organic matter in WK-A (51%) and WK-P (58%) was preferentially associated with fine soil aggregates with aggregate size <231 μm. Those fine soil aggregates only contribute 26% and 40% to the total soil mass in WK-A and WK-P, respectively. Increasing of SOM in the fine aggregate size fractions (Table 1) confirms that SOM is preferentially increased in small aggregates with high surface area to mass ratios. Compared to the WK-A, much higher SOM concentrations were observed in the WK-P paddy soils, which may indicate that rice planting may potentially increase the organic matter content of the soils. Indeed, increases in SOM have been observed in paddy field soils that have been in cultivation for 30–100 years in Japan and China (Mitsuchi, 1974). Flooding of rice paddy minimizes the exposure of soil to air, which tends to retain organic matters in soil (Tisdall and Oades, 1982). Long-term dry land cropping can expose more soil to the air, during which the organic matter in soil is decomposed to carbon dioxide (Haynes and Francis, 1993).

4.2. Distribution of total Hg content in soils

Soils from both WK-A and WK-P show much higher THg in fine soil aggregate size fractions (Fig. 3C). Minerals in soils are mainly classified as primary and secondary minerals. Primary minerals (such as quartz, feldspars, etc), which have not experienced significant chemical or structural alteration since their crystallization within the parent rocks, are usually found in the relatively less weathered large soil aggregates. Secondary minerals (such as clay minerals, goethite, and hematite), mainly the weathering products of primary minerals, are often enriched in fine soil aggregates. Secondary minerals in soils have shown larger specific surface area and higher adsorption capacity than primary minerals (Hardy and Cornu, 2006). The relative enrichment of THg in fine soil fractions may be attributed to the higher content of secondary minerals. Another possible explanation for enrichment of Hg in fine soil fractions is provided by Kim et al. (2004), who demonstrated that Hg-sulfides are insoluble yet mineralogically soft, and can preferentially weather into finer soil fractions. Further, the enrichment of Hg in fine fractions may be explained by SOM, consistent with other studies of organic matter in soils, peats, and sediments (Yin et al., 1996; Skyllberg et al., 2000; Schuster, 1991). Mercury has a strong affinity to S-containing functional groups which are frequently found in soil organic matters (Skyllberg, 2008). Fine soil fractions in both WK-A and WK-P show relatively higher THg concentrations (Fig. 3B). In all soil fractions in WK-A ($r = 0.82$, $p = 0.02$) and WK-P ($r = 0.89$, $p = 0.02$), THg showed significantly positive correlations with the SOM (Fig. 4), suggesting the close association between Hg and SOM in WMMD soils. Compared to WK-A, much higher THg/SOM ratios were observed in WK-P soils, partly attributed to the higher reactive surface area of the more humified organic matter in paddy soils (Pramanik and Kim, 2014). Studies have reported that Hg–SOM complexes can reconcile with the abundance of HgS (Ravichandran et al., 1999; Skyllberg, 2008; Skyllberg et al., 2000; Skyllberg and Drott, 2010; Deonarine and Hsu-Kim, 2009; Manceau et al., 2015). Studies also reported changing THg/SOM ratios in soils, are the result of historical Hg loading rates and the quality of SOM in soils in the different sites of the same area (Lindqvist et al., 1991; Grigal, 2003).

4.3. Hg speciation in soils under different cultivations

As shown in Table 1, our results indicate that β-HgS is the primary Hg species (WK-A: 69–81%; WK-P: 64–73%). Other than two samples in WK-P (231–180 μm: 16.4%; <75 μm: 11.6%), most soils in WK-A and WK-P show the α-HgS fraction is lower than the analytical error (10%). Our previous data showed that α-HgS (99%) is the primary Hg species in Hg ores of WMMD, whereas the major Hg species in waste calcines are α-HgS (52%) and β-HgS (42%) (Yin et al., 2013a). The lack of α-HgS in WMMD soils may suggest lower mobility of α-HgS from Hg mine wastes to WMMD soils, supported by the low solubility of α-HgS (Rimondi et al., 2014). The fractions of β-HgS in WK-A (69–81%) and WK-P (64–73%) are much higher than that in unroasted Hg ore (mainly α-HgS) and roasted waste calcine (52%) in WMMD. β-HgS is the low-temperature polymorph of HgS (Gerbig et al., 2011). Like α-HgS (solubility: 10^{-54}), β-HgS (10^{-52}) also have a low solubility under oxic, abiotic conditions (Faure, 1991). It is unlikely that the mobilization of β-HgS in Hg calcines can lead to the high proportion of β-HgS in the WMMD soils. Another possible explanation for high β-HgS could beits formation in soils. β-HgS has been found to be the most common form in highly Hg-contaminated floodplains and soils (Ravichandran et al., 1999; Benoit et al., 2001; Slowey, 2010; Skyllberg and Drott, 2010). Interactions of dissolved Hg(II) with dissolved organic matter (DOM) have been shown to form β-HgS (Skyllberg and Drott, 2010). Ravichandran et al. (1999) observed that humic fractions (humic, fulvic, hydrophobic, and hydrophilic acids) of DOM inhibited the precipitation and aggregation of β-HgS. The positive relations of Hg and SOM (Fig. 3)

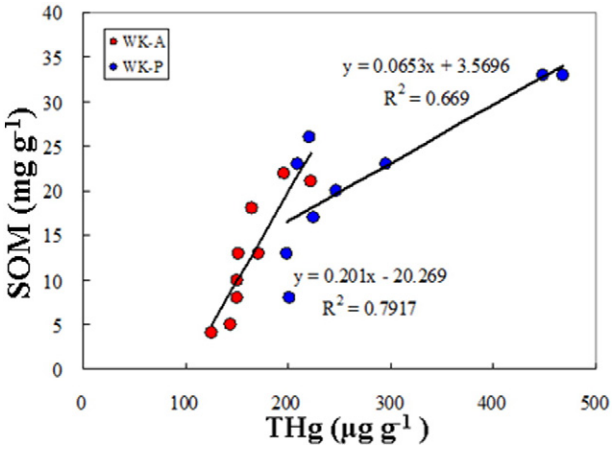

Fig. 4. Correlations between THg and SOM contents of the sieved soil fractions from sites in the Wanshan Mercury Mining District.

and the higher fractions of β-HgS in WMMD soils showed evidence that a substantial amount of β-HgS can be formed in highly Hg contaminated soils.

At WMMD, leaching of Hg mine waste has been shown to contain high concentrations of Hg(II), which mainly form by dissolution of by-product Hg species (Li et al., 2013). Detectable (>10%) of $HgCl_2$ was observed in some soils at WK-A (231–180 μm: 12.5%; 125–105 μm: 10.3%; 105–90 μm: 12.7%; 90–75 μm: 10.7%; <75 μm: 10.4%). As $HgCl_2$ has relatively high solubility (Faure, 1991), our observation of $HgCl_2$ in WMMD soils may be due $HgCl_2$ leaching from the waste calcine. An alternative explanation is that $HgCl_2$ may form from more mobile/dissolved forms of Hg in WMMD soils, perhaps due to elevated salt [thus Cl(-II)] levels in the soils compared to the waste calcines. Soluble Hg species (e.g., $HgCl_2$) in soils may interact with DOM and form β-HgS (Ravichandran et al., 1999; Benoit et al., 2001; Slowey, 2010; Skyllberg and Drott, 2010). Other than two samples in WK-A (105–90 μm: 9.5%) and WK-P (389–231 μm: 4.4%), most samples in WMMD show significant proportion of Hg(0) (>10%). Our data is consistent with the EXAFS results by Rimondi et al. (2014), who observed Hg(0) in sediments collected from Mt. Amiata Hg mining district in Italy. In WMMD, the presence of Hg(0) in soils can be explained by deposition of gaseous Hg(0) that is emitted from Hg mining activities or from the tailings as evidenced by high levels of gaseous elemental Hg (up to 1108 ng m^{-3}) in the WMMD region (Wang et al., 2007). Soluble Hg species (e.g., $HgCl_2$) in soils can also be readily reduced to Hg(0) during various biotic (e.g., microbially-mediated reduction) and abiotic processes (Kritee et al., 2007).

5. Conclusion

Our study has shown that different cultivation (rice paddy, arid land cropping) can lead to large differences in soil aggregate size distributions and SOM contents, which control the distribution of Hg in soils. Small soil aggregates are generally characterized by higher SOM content and higher Hg concentration. Rice cultivation not only reduces the relative proportion of larger soil aggregates, but also tends retain SOM by a potential minimization of the exposure to air. As a result, Hg concentrations in paddy soil may be increased during long-term rice cultivation. In WMMD, soils primarily contain β-HgS. Soluble Hg species (e.g., $HgCl_2$) interacting with soil DOM may be the main source of β-HgS in these soils. The presence of minor amounts of $HgCl_2$ and Hg(0) in soils also represents a considerable environmental concern of WMMD, because these Hg species are more bioavailable for Hg methylation (Barkay et al., 1997) and subsequent bioaccumulation.

Acknowledgments

This study was supported by the National Key Basic Research Program of China (2013CB430004) and the National Natural Science Foundation of China (41303014, 41173024). Two anonymous reviewers and editor Edward A. Nater are acknowledged for their constructive comments and useful suggestions.

References

Akagi, H., Nishimura, H., 1991. Speciation of Mercury in the Environment. Advances in Mercury Toxicology. Springer, US, pp. 53–76.
Arshad, M.A., Coen, G.M., 1992. Characterization of soil quality: physical and chemical criteria. Am. J. Altern. Agric. 7 (1–2), 25–31.
Bao, Z., Feng, X., Wang, J., 2011. Distribution of mercury speciation in polluted soils of Wanshan mercury mining area in Guizhou. Chin. J. Ecol. 30 (5), 907–913 (In Chinese with English abstract).
Barkay, T., Gillman, M., Turner, R.R., 1997. Effects of dissolved organic carbon and salinity on bioavailability of mercury. Appl. Environ. Microbiol. 1997 (63), 4267–4271.
Benoit, J.M., Mason, R.P., Gilmour, C.C., et al., 2001. Constants for mercury binding by dissolved organic matter isolates from the Florida Everglades. Geochim. Cosmochim. Acta 65 (24), 4445–4451.
Biester, H., Gosar, M., Müller, G., 1999. Mercury speciation in tailings of the Idrija mercury mine. J. Geochem. Explor. 65 (3), 195–204.
Chadwick, S.P., Babiarz, C.L., Hurley, J.P., et al., 2013. Importance of hypolimnetic cycling in aging of "new" mercury in a northern temperate lake. Sci. Total Environ. 448, 176–188.
Deonarine, A., Hsu-Kim, H., 2009. Precipitation of mercuric sulfide nanoparticles in NOM-containing water: implications for the natural environment. Environ. Sci. Technol. 43, 2368–2373.
Dexter, A.R., 1988. Advances in characterization of soil structure. Soil Tillage Res. 11 (3), 199–238.
Farella, N., Davidson, R., Lucotte, M., et al., 2007. Nutrient and mercury variations in soils from family farms of the Tapajós region (Brazilian Amazon): recommendations for better farming. Agric. Ecosyst. Environ. 120 (2), 449–462.
Faure, G., 1991. Principles and Applications of Geochemistry. Prentice Hall, Upper Saddle River.
Fernández-Martínez, R., Loredo, J., Ordóñez, A., et al., 2006. Physicochemical characterization and mercury speciation of particle-size soil fractions from an abandoned mining area in Mieres, Asturias (Spain). Environ. Pollut. 142 (2), 217–226.
Gee, G.W., Bauder, J.W., 1986. Particle-size analysis. In: Klute, A. (Ed.), Methods of Soil Analysis. Part 1, second ed. Agron. Monogr. 9. ASA and SSSA, Madison, WI, pp. 383–411.
Gerbig, C.A., Kim, C.S., Stegemeier, J.P., et al., 2011. Formation of nanocolloidal metacinnabar in mercury–DOM–sulfide systems. Environ. Sci. Technol. 45 (21), 9180–9187.
Gray, J.E., Hines, M.E., Biester, H., 2006. Mercury methylation influenced by areas of past mercury mining in the Terlingua district, Southwest Texas, USA. Appl. Geochem. 21 (11), 1940–1954.
Gray, J.E., Hines, M.E., Higueras, P.L., Adatto, I., Lasorsa, B.K., 2004. Mercury speciation and microbial transformations in mine wastes, stream sediments, and surface waters at the Almadén mining district, Spain. Environ. Sci. Technol. 38 (16), 4285–4292.
Grigal, D.F., 2003. Mercury sequestration in forests and peatlands. J. Environ. Qual. 32 (2), 393–405.
Hardy, M., Cornu, S., 2006. Location of natural trace elements in silty soils using particle-size fractionation. Geoderma 133 (3), 295–308.
Haynes, R.J., Francis, G.S., 1993. Changes in microbial biomass C, soil carbohydrate composition and aggregate stability induced by growth of selected crop and forage species under field conditions. J. Soil Sci. 44 (4), 665–675.
Hussain, I., Olson, K.R., Wander, M.M., Karlen, D.L., 1999. Adaptation of soil quality indices and application to three tillage systems in Southern Illinois. Soil Tillage Res. 50 (3–4), 237–249.
Jew, A.D., Kim, C.S., Rytuba, J.J., Gustin, M.S., Brown Jr., G.E., 2010. New technique for quantification of elemental Hg in mine wastes and its implications for mercury evasion into the atmosphere. Environ. Sci. Technol. 45 (2), 412–417.
Jiang, G.B., Shi, J.B., Feng, X.B., 2006. Mercury pollution in China. Environ. Sci. Technol. 40 (12), 3672–3678.
Kelly, C.A., Rudd, J.W.M., Bodaly, R.A., et al., 1997. Increases in fluxes of greenhouse gases and methyl mercury following flooding of an experimental reservoir. Environ. Sci. Technol. 31 (5), 1334–1344.
Kim, C.S., Brown Jr., G.E., Rytuba, J.J., 2000. Characterization and speciation of mercury-bearing mine wastes using X-ray absorption spectroscopy. Sci. Total Environ. 261 (1), 157–168.
Kim, C.S., Rytuba, J.J., Brown Jr., G.E., 2004. Geological and anthropogenic factors influencing mercury speciation in mine wastes: an EXAFS spectroscopy study. Appl. Geochem. 19 (3), 379–393.
Kritee, K., Blum, J.D., Johnson, M.W., et al., 2007. Mercury stable isotope fractionation during reduction of Hg(II) to Hg(0) by mercury resistant microorganisms. Environ. Sci. Technol. 41 (6), 1889–1895.
Li, P., Feng, X.B., Qiu, G.L., et al., 2009. Mercury pollution in Asia: a review of the contaminated sites. J. Hazard. Mater. 168 (2), 591–601.
Li, P., Feng, X., Qiu, G., et al., 2013. Mercury speciation and mobility in mine wastes from mercury mines in China. Environ. Sci. Pollut. Res. 20 (12), 8374–8381.
Lindqvist, O., Johansson, K., Bringmark, L., et al., 1991. Mercury in the Swedish environment—recent research on causes, consequences and corrective methods. Water Air Soil Pollut. 55 (1–2), xi–261.
Lv, J., Luo, L., Zhang, J., et al., 2012. Adsorption of mercury on lignin: combined surface complexation modeling and X-ray absorption spectroscopy studies. Environ. Pollut. 162, 255–261.
Manceau, A., Lemouchi, C., Enescu, M., et al., 2015. Formation of mercury sulfide from Hg(II)–thiolate complexes in natural organic matter. Environ. Sci. Technol. http://dx.doi.org/10.1021/acs.est.5b02522.
Mitsuchi, M., 1974. Pedogenic characteristics of paddy soils and their significance in soil classification. Bull. Natl. Inst. Agric. Sci. Ser. B Soils Fertil.
Moormann, F.R., Breemen, N.V., 1978. Rice: soil, water, land. Rice: soil, water, land. Rice Res. Inst.
Nelson, D.W., Sommers, L.E., 1982. Total carbon, organic carbon, and organic matter. Methods of soil analysis. Part 2. Chemical and Microbiological Properties, pp. 539–579.
Newville, M., 2001. IFEFFIT: interactive XAFS analysis and FEFF fitting. J. Synchrotron Radiat. 8 (2), 322–324.
Pramanik, P., Kim, P.J., 2014. Fractionation and characterization of humic acids from organic amended rice paddy soils. Sci. Total Environ. 466, 952–956.
Qiu, G., Feng, X., Wang, S., Shang, L., 2005. Mercury and methylmercury in riparian soil, sediments, mine-waste calcines, and moss from abandoned Hg mines in east Guizhou province, southwestern China. Appl. Geochem. 20 (3), 627–638.
Qiu, G., et al., 2008. Methylmercury accumulation in rice (*Oryza sativa* L.) grown at abandoned mercury mines in Guizhou, China. J. Agric. Food Chem. 56 (7), 2465–2468.
Ravichandran, M., Aiken, G.R., Ryan, J.N., et al., 1999. Inhibition of precipitation and aggregation of metacinnabar (mercuric sulfide) by dissolved organic matter isolated from the Florida Everglades. Environ. Sci. Technol. 33 (9), 1418–1423.

Rimondi, V., et al., 2014. Mercury speciation in the Mt. Amiata mining district (Italy): interplay between urban activities and mercury contamination. Chem. Geol. 380, 110–118.
Rothenberg, S.E., Feng, X., Dong, B., et al., 2011. Characterization of mercury species in brown and white rice (*Oryza sativa* L.) grown in water-saving paddies. Environ. Pollut. 159 (5), 1283–1289.
Roulet, M., Lucotte, M., Farella, N., et al., 1999. Effects of recent human colonization on the presence of mercury in Amazonian ecosystems. Water Air Soil Pollut. 112 (3–4), 297–313.
Roulet, M., Lucotte, M., Saint-Aubin, A., et al., 1998. The geochemistry of mercury in central Amazonian soils developed on the Alter-do-Chao formation of the lower Tapajos River Valley, Para state, Brazil. Sci. Total Environ. 223 (1), 1–24.
Schmidt, M.W.I., Kögel-Knabner, I., 2002. Organic matter in particle-size fractions from A and B horizons of a Haplic Alisol. Eur. J. Soil Sci. 53 (3), 383–391.
Schuster, E., 1991. The behavior of mercury in the soil with special emphasis on complexation and adsorption processes—a review of the literature. Water Air Soil Pollut. 56 (1), 667–680.
Skyllberg, U., Drott, A., 2010. Competition between disordered iron sulfide and natural organic matter associated thiols for mercury(II)—an EXAFS study. Environ. Sci. Technol. 44 (4), 1254–1259.
Skyllberg, U., 2008. Competition among thiols, inorganic sulfides and polysulfides for Hg and MeHg in wetland soils and sediments under suboxic conditionssillumination of controversies and implications for MeHg net production. J. Geophys. Res. 113, G00C03.
Skyllberg, U., Xia, K., Bloom, P.R., Nater, E.A., Bleam, W.F., 2000. Binding of mercury (II) to reduced sulfur in soil organic matter along upland-peat soil transects. J. Environ. Qual. 29 (3), 855–865.
Slowey, A.J., 2010. Rate of formation and dissolution of mercury sulfide nanoparticles: the dual role of natural organic matter. Geochim. Cosmochim. Acta 74 (16), 4693–4708.
Stein, E.D., Cohen, Y., Winer, A.M., 1996. Environmental distribution and transformation of mercury compounds. Crit. Rev. Environ. Sci. Technol. 26 (1), 1–43.
Tisdall, J.M., Oades, J.M., 1982. Organic matter and water-stable aggregates in soils. J. Soil Sci. 33 (2), 141–163.
US Environmental Protection Agency, 2011. Human health medium specific screening levels. http://www.epa.gov/region6/6pd/rcra_c/pd-n/screen.htm (Accessed 16 June 2013.
Utomo, W.H., Dexter, A.R., 1981. Soil friability. J. Soil Sci. 32 (2), 203–213.
Wang, S., Feng, X., Qiu, G., et al., 2007. Characteristics of mercury exchange flux between soil and air in the heavily air-polluted area, eastern Guizhou, China. Atmos. Environ. 41 (27), 5584–5594.
Yin, R., Feng, X., Meng, B., 2013c. Stable mercury isotope variation in rice plants (*Oryza sativa* L.) from the Wanshan mercury mining district, SW China. Environ. Sci. Technol. 47 (5), 2238–2245.
Yin, R., Feng, X., Wang, J., et al., 2013a. Mercury speciation and mercury isotope fractionation during ore roasting process and their implication to source identification of downstream sediment in the Wanshan mercury mining area, SW China. Chem. Geol. 336, 72–79.
Yin, R., Feng, X., Wang, J., et al., 2013b. Mercury isotope variations between bioavailable mercury fractions and total mercury in mercury contaminated soil in Wanshan Mercury Mine, SW China. Chem. Geol. 336, 80–86.
Yin, R., Feng, X., Li, X., et al., 2014. Trends and advances in mercury stable isotope system as a geochemical tracer. Trends Environ. Anal. Chem. 2, 1–10.
Yin, R., Feng, X., Li, Z., et al., 2012. Metallogeny and environmental impact of Hg in Zn deposits in China. Appl. Geochem. 27 (1), 151–160.
Yin, Y., Allen, H.E., Li, Y., et al., 1996. Adsorption of mercury(II) by soil: effects of pH, chloride, and organic matter. J. Environ. Qual. 25 (4), 837–844.
Zhang, G., Liu, C.Q., Wu, P., et al., 2004. The geochemical characteristics of mine-waste calcines and runoff from the Wanshan mercury mine, Guizhou, China. Appl. Geochem. 19 (11), 1735–1744.
Zhang, H., Feng, X., Larssen, T., et al., 2010. In inland China, rice, rather than fish, is the major pathway for methylmercury exposure. Environ. Health Perspect. 118 (9), 1183–1188.